Biomaterials 257 (2020) 120238

Contents lists available at ScienceDirect

Biomaterials

journal homepage: www.elsevier.com/locate/biomaterials

Enzymatic protection and biocompatibility screening of enzyme-loaded polymeric nanoparticles for neurotherapeutic applications

Rick Liao [a], Jessica Pon [a], Michael Chungyoun [a], Elizabeth Nance [a,b,c,*]

[a] Department of Chemical Engineering, University of Washington, Seattle, WA, USA
[b] Department of Radiology, University of Washington, Seattle, WA, USA
[c] Center on Human Development and Disability, University of Washington, Seattle, WA, USA

ARTICLE INFO

Keywords:
PLGA
PEG
Double emulsion
Nanoprecipitation
Dichloromethane
Sonication

ABSTRACT

Polymeric nanoparticles provide a non-invasive strategy for enhancing the delivery of labile hydrophilic enzymatic cargo for neurological disease applications. One of the most common polymeric materials, poly(lactic-co-glycolic acid) (PLGA) copolymerized with poly(ethylene glycol) (PEG) is widely studied due to its biocompatible and biodegradable nature. Although PLGA-PEG nanoparticles are generally known to be non-toxic and protect enzymatic cargo from degradative proteases, different formulation parameters including surfactant, organic solvent, sonication times, and formulation method can all impact the final nanoparticle characteristics. We show that 30s sonication double emulsion (DE)-formulated nanoparticles achieved the highest enzymatic activity and provided the greatest enzymatic activity protection in degradative conditions, while nanoprecipitation (NPPT)-formulated nanoparticles exhibited no protection compared to free catalase. However, the same DE nanoparticles also caused significant toxicity on excitotoxicity-induced brain tissue slices, but not on healthy or neuroinflammation-induced tissue. We narrowed the culprit of toxicity to specifically sonication of PLGA-PEG polymer with dichloromethane (DCM) as the organic solvent, independent of surfactant type. We also discovered that toxicity was oxidative stress-dependent, but that increased toxicity was not enacted through increasing oxidative stress. Furthermore, no PEG degradation or aldehyde, alcohol, or carboxylic acid functional groups were detected after sonication. We identified that inclusion of free PEG along with PLGA-PEG polymer during the emulsification phases or replacing DCM with trichloromethane (chloroform) produced biocompatible polymeric nanoparticle formulations that still provided enzymatic protection. This work encourages thorough screening of nanoparticle toxicity and cargo-protective capabilities for the development of enzyme-loaded polymeric nanoparticles for the treatment of disease.

1. Introduction

Polymeric nanoparticles have been extensively researched for drug delivery applications to the central nervous system due to their ability to overcome physiological barriers, exhibit controlled release, and alter drug metabolism and clearance kinetics [1–3]. Therapeutic-encapsulating polymeric nanoparticles can provide stability and protection for enzymatic cargo from proteolytic conditions and can traverse the blood-brain barrier (BBB) [4,5]. One of the most common polymeric materials is the copolymer poly(lactic-*co*-glycolic acid) (PLGA) due to its biocompatibility and biodegradability [6–8]. PLGA nanoparticles are capable of carrying a variety of hydrophobic or hydrophilic therapeutic cargo within their polymer matrix core, including small molecule drugs and macromolecules such as proteins or DNA [9]. Formulating PLGA nanoparticles with a dense poly(ethylene glycol) (PEG) coating can imbue stealth-like properties for the avoidance of reticuloendothelial system detection and enhance brain tissue penetration while retaining biocompatibility [6,10]. For PLGA-PEG block copolymer, the most common nanoparticle formulation approaches are the emulsion solvent evaporation (double emulsion (DE) for hydrophilic cargo), nanoprecipitation (NPPT), also known as solvent displacement, and salting out methods [6,9].

Therapeutic enzymes are of special interest due to their precise catalytic functions, but oral and intravenous administration of free enzymes have had limited success due to proteolytic degradation and poor brain biodistribution [11]. Attempts to overcome these issues include

* Corresponding author. Department of Chemical Engineering, University of Washington, Seattle, WA, USA.
E-mail address: eanance@uw.edu (E. Nance).

https://doi.org/10.1016/j.biomaterials.2020.120238
Received 11 May 2020; Received in revised form 12 July 2020; Accepted 13 July 2020
Available online 15 July 2020
0142-9612/

administering greater drug concentrations that exceed proteolysis rates, and covalent conjugation of ligands to the enzyme for enhanced targeting [4,12,13]. However, even if enzymes survive the journey into and through systemic circulation, 100% of large therapeutic molecules fail to cross the intact BBB [14]. Altogether, these obstacles demand the use of drug-carrier vehicles such as polymeric PLGA-PEG nanoparticles to effectively deliver enzyme therapeutics. PLGA-PEG nanoparticles can be incorporated into biocompatible two-dimensional transition metal dichalcogenides or hydrogel scaffolds to further tailor therapeutic release strategies [15,16].

Despite the fact that PLGA-PEG nanoparticles are known to be biocompatible and protective of enzymatic cargo, similar formulation conditions do not guarantee the same advantageous characteristics. Thus, each distinct formulation should be appropriately screened to ensure enzyme protection and biocompatibility in various environments representative of the *in vivo* landscape. Failure to do so could lead to an enzyme-encapsulating nanoparticle falling short in clinical trials due to ineffective enzyme protection, or worse, due to inadvertent toxicity exacerbating the disease outcome. Here, we compare DE and NPPT nanoparticle formulations and show varying efficacy in protecting enzymatic activity. Using organotypic whole hemisphere (OWH) brain slice models of neurological disease as a tool for toxicity screening of nanoparticle formulations, we discovered the toxicity of PLGA-PEG DE nanoparticles formulated with dichloromethane (DCM) organic solvent on excitotoxicity-induced brain environments. We further used the OWH models to identify alternative formulation conditions that exhibit biocompatibility and retain enzymatic protection.

2. Materials and methods

2.1. Nanoparticle formulation and characterization

The water 1/organic/water 2 ($w_1/o/w_2$) DE was used for enzyme encapsulation. One mg enzyme was dissolved in 100 μL 1x phosphate buffered saline (PBS, Corning) and combined with 100 μL of 1 wt% cholic/deoxycholic acid (CHA) sodium salt (bile salts, Sigma) or 1 wt% polyvinyl alcohol (PVA, Sigma) surfactant dissolved in deionized water (DI) for w_1 phase. The w_1 aqueous phase was combined with 25 mg of PLGA (45k, LA:GA 50:50) copolymerized with PEG (5k) (Akina) dissolved in 1 mL dichloromethane (DCM, Fisher Scientific), ethyl acetate (EtAc, Avantor), or trichloromethane/chloroform (TCM, Fisher Scientific) for organic phase and emulsified with a Sonic Dismembrator Ultrasonic Processor (Fisher Scientific). The slightly miscible, but incompatible w_1/o phases were emulsified by 20 kHz probe sonication at 30% amplitude with 1s on:1s off pulses for 1s, 15s, 30s, or 60s on. After adding 4 mL 3% CHA or 5% PVA in deionized water (DI) as the w_2 phase, the second sonication was performed at 20% amplitude with 1s on:1s off pulses for the same length of time. This emulsion was then poured into a 500-rotations per minute (rpm) stirred 25 mL beaker of PBS (sink) for organic solvent evaporation. After 3 h, the nanoparticles were collected with a 1h 100k relative centrifugal unit (RCF) centrifugation step, followed by 5 mL PBS resuspension, 30 m 100k RCF centrifugation, and final resuspension in 1 mL PBS. To remove aggregates, the nanoparticle solution was transferred to a new tube after 10 s of mini benchtop centrifugation and stored at 4C until further usage. Nanoparticles were measured with a Malvern Zetasizer for hydrodynamic diameter and zeta-potential (ζ-potential). For a subset of DE formulations, 25 mg of PLGA (45k LA:GA 50:50) (Akina) was used instead of PLGA-PEG, or 5 mg methoxy-PEG with a hydroxyl terminus (mPEG-OH, Creative PEGWorks) was dissolved either in the DCM, in the sink phase, or in the PBS final resuspension phase.

For the NPPT method, 1 mg enzyme was dissolved in 100 μL PBS and combined with 400 μL 1% CHA or PVA in DI, and 25 mg PLGA-PEG polymer was dissolved in 500 μL acetone. After combining and vortex mixing the aqueous and organic phases for 2 s, the solution was added dropwise with a 1 mL Hamilton syringe (Hamilton) to 25 mL beaker of PBS. Nanoparticles were collected via the same methodology as above for DE method.

2.2. Catalase activity assay

Catalase (catalase from bovine liver, Sigma) was used as a model enzyme due to its facile enzymatic activity measurement using a catalase spectrophotometric assay adapted from Beers and Sizer [17]. A pH 7.0 solution of 0.036% w/w H_2O_2 (Sigma) was prepared in 50 mM phosphate buffer (PB) with a 240-nm absorbance (A_{240}) between 0.48 and 0.52. In an optically clear quartz cuvette (Hellma Analytics), 100 μL of catalase sample was added to 2.9 mL of H_2O_2 solution, mixed via pipetting, and A_{240} was measured at 1s intervals for 3 min using a kinetic spectrometric reading on a SpectraMax M5 UV–Vis Spectrophotometer (Molecular Devices). The active units per mg of catalase were calculated using Equation (2):

$$\frac{Units}{mg\ solid} = \frac{\frac{(3.45)(df)}{(time)(0.1)}}{\frac{mg\ solid}{mL\ enzyme}} \quad (2)$$

In the equation, 3.45 represents the decomposition of 3.45 μmoles of H_2O_2 during A_{240} decrease from 0.45 to 0.4, df is the dilution factor of the sample, and 0.1 is the mL volume of sample added. This assay measures catalase activity even when the enzyme is encapsulated, due to the ability of H_2O_2 to diffuse throughout the polymer matrix [4]. Stock catalase had 2000-3000 active units (AU) per mg of catalase.

2.3. Bicinchoninic acid (BCA) protein concentration assay

100 μL of catalase-loaded nanoparticles was combined with 50 μL of 1 M sodium hydroxide (ThermoFisher). The solution was vortexed for 2s, spun down on a minicentrifuge, and then incubated at 37 °C for 30 min for base-catalyzed hydrolysis of the PLGA polymer to release all loaded catalase. 50 μL PBS was then added to neutralize the solution. The sample was then tested for protein concentration with the Pierce BCA Protein Assay Kit (ThermoFisher). Following the manufacturer's instructions, 25 μL sample was added to 96-well plate in triplicate on ice. After addition of 200 μL BCA assay working reagent (50:1 reagent A:B), the plate was placed on a shaker plate at 37 °C for 30 min. After 30 min, the plate was placed on ice, and absorbance was measured at 562 nm on a SpectraMax M5 UV–Vis Spectrophotometer (Molecular Devices).

2.4. Scanning electron microscopy (SEM)

For CHA 1s and 30s DE and NPPT nanoparticle formulation conditions, nanoparticle samples were further processed for scanning electron microscopy. After the final centrifugation, nanoparticles were resuspended in DI instead of PBS and diluted 100x in 200 proof ethanol (Decon Labs). Subsequently, 100 μL of the diluted nanoparticle solutions were pipetted onto a silicon wafer and allowed to air-dry for 1h in a fume hood. The nanoparticles were sputter coated with palladium under an argon environment and imaged on the FEI XL830 Dual Beam Focused Ion Beam/Scanning Electron Microscope in the UW Molecular Analysis Facility.

2.5. Animal work and ethics statement

This study was performed in strict accordance with the recommendations in the Guide for the Care and Use of Laboratory Animals of the National Institutes of Health. All of the animals were handled according to approved institutional animal care and use committee (IACUC) protocols (**#4383-02**) of the University of Washington. The University of Washington has an approved Animal Welfare Assurance (#A3464-01) on file with the NIH Office of Laboratory Animal Welfare (OLAW), is registered with the United States Department of Agriculture (USDA, certificate #91-R-0001), and is accredited by AAALAC International.

Every effort was made to minimize suffering, stress, or pain.

2.6. Preparation for OWH brain slice culturing

OWH brain slice cultures were prepared following the same methodology as previously published [18]. On postnatal (P) day 14, healthy female Sprague Dawley rats were injected intraperitoneally with 100 μL pentobarbital, followed by rapid decapitation with surgical scissors once the body is non-responsive. After removing the brain, under sterile conditions, the brain was split into hemispheres with a sterile razor blade and sliced into 300 μm sections with a McIlwain tissue chopper (Ted Pella). Brain slices were separated in dissecting media (0.64% w/v glucose, 100% HBSS (Hank's Balanced Salt Solution), 1% penicillin). Brain slices containing the hippocampus were transferred onto 35-mm 0.4-μm-pore-sized membrane inserts (Millipore), and placed within a non-treated 6-well plate (CytoOne) containing 1 mL 37 °C pre-heated slice culture media (SCM, 50% MEM (minimum essential media), 50% HBSS, 1% GlutaMAX, and 1% penicillin). All media added to slices was pre-warmed at 37 °C. MEM was purchased from Life Technologies, glucose from Sigma, and HBSS, GlutaMAX, and penicillin from Gibco. The slices rested overnight in a CO_2 incubator (ThermoFisher) at 37 °C with constant humidity, 95% air, and 5% CO_2 to equilibrate after the mechanical stress of slicing before continuing experiments.

2.7. OWH sample preparation for LDH cytotoxicity

After slices rest overnight, supernatant was collected (time t = -3h) and replaced with SCM, SCM with 1 μg/mL lipopolysaccharide (LPS, Sigma), SCM with 1000 mM monosodium glutamate (MSG, Sigma), or oxygen and glucose deprived (OGD) SCM for disease induction if applicable. OGD SCM consisted of 150 mM sodium chloride (NaCl, Sigma), 2.8 mM potassium chloride (KCl, Sigma), 1 mM calcium chloride ($CaCl_2$, Sigma), and 10 mM 4-(2-hydroxyethyl)piperazine-1-ethanesulfonic acid buffer solution (HEPES, Gibco) in DI titrated to pH 7.4 with 1 M hydrochloric acid (ThermoFisher) or 1 M sodium hydroxide (ThermoFisher), and bubbled with nitrogen gas (Praxair) for 10 min. For OGD-exposed slices, the 6-well plate was placed in a Hypoxia Incubator Chamber (STEMCELL Technologies) and placed in 37 °C incubator. The chamber was flushed with nitrogen gas (Praxair) for 10 min, followed by clamping of the tubing, and continued slice incubation for the rest of the 3h. For slice culturing studies, the end of the 3h incubation was defined as time t = 0h. At t = 0h, the supernatant was collected and replaced with normal SCM. At t = 0h, 100 μL PBS containing nanoparticles, surfactant, 0.1 mg superoxide dismutase (SOD, Cu/Zn SOD1 from bovine erythrocytes, Sigma), or pure SCM as a control, was gently added to the top of the brain slice using a cut-tip pipet. Supernatant collection and media replacement were repeated at time 1h, 2h, 4h, 8h, and 24h. All supernatant samples were immediately stored in −80 °C. SCM without any additional toxins served as the non-treated (NT) control. NT control slices were incubated with NT SCM throughout the 3h incubation and 24h culturing.

Supernatant samples were removed and thawed at room temperature (RT) to conduct lactate dehydrogenase (LDH) assays (601170, Cayman Chemical). Following the manufacturer's instructions, 100 μL of sample supernatant was added to 100 μL of LDH reaction buffer in triplicate to 96-well plates on ice, and the plates were transferred to a stir plate in a 37 °C incubator. After 30 min, the plates were placed on ice, and absorbance was measured at 490 nm (A_{490}) on a SpectraMax M5 UV–Vis Spectrophotometer (Molecular Devices) to detect the production of colorimetric formazan. Percent cytotoxicity was calculated using Equation (1).

$$\%cytotoxicity = \frac{cumulative\ LDH\ abs\ of\ sample}{24h\ cumulative\ LDH\ abs\ of\ 1000\ mM\ MSG\ sample} \times 100\% \quad (1)$$

2.8. OWH immunofluorescence staining and imaging

At t = 24h, a subset of slices was stained with 1 mL SCM with 5 μg/mL propidium iodide (PI) in SCM for 1h at culturing conditions. Slices were washed twice for 1 min with SCM, followed by a 1h wash with SCM at culturing conditions. OWH brain slices were fixed in 10% formalin (10% phosphate buffered formalin, ThermoFisher) with 1 mL below membrane insert and 500 μL directly on the slice at room temperature for 1 h. Slices were washed twice with PBS and stored in 1 mL PBS until further staining. Recombinant antibodies for neurons (rabbit anti-MAP2, Abcam) were prepared 1:250 in PBS with 0.3% TX (PBS+) and 6% goat serum (Sigma) (PBS-g++). 250 μL primary antibody solutions were added to each tissue section for 6h at room temperature. Sections were washed twice in PBS. Secondary antibodies for neurons (Alexa Fluor (AF)-488 IgG goat anti-rabbit, Invitrogen) were prepared 1:500 in PBS+, and 250 μL secondary antibody solutions were added to each tissue section for 2h and washed twice in PBS. Sections were stained with 1 mL of 1:1000 4′,6-diamidino-2-phenylindole (DAPI, Invitrogen) in PBS for 15 min, washed twice in PBS, and then stored in PBS at 4 °C until imaged on a Nikon confocal microscope. 40x confocal images were obtained for MAP2 (neurons), PI (dead/dying nuclei), and DAPI (all nuclei) imaging.

2.9. Serum collection from rats

Adult rats were injected intraperitoneally with an overdose of 120–150 mg/kg of pentobarbital (Commercial Beuthanasia D, 390 mg/mL pentobarbital). Immediately after death, the chest cavity was opened to expose the heart, upon which a 22g needle syringe (BD) was used to puncture the left ventricle for blood draw. Blood was transferred to 1.5 mL microcentrifuge tubes and incubated for 60 min at room temperature to permit coagulation. The tubes containing coagulated blood were spun at 2k RCF for 10 min at 4 °C. Serum was transferred to a separate tube and immediately stored at −80 °C. Serum samples were thawed and mixed with free catalase or used for resuspending nanoparticles, and then assayed for catalase activity as described above.

2.10. Catalase activity stability study

For the catalase activity stability studies, free catalase or catalase-loaded nanoparticles were stir-incubated in PBS with 0.2 wt% pronase (pronase from *Streptomyces griseus*, Sigma) or in rat serum at 37 °C. For the activity stability studies with pronase, at 0h, 1h, 2h, 4h, 8h, and 24h, aliquots were collected, placed on ice, and immediately tested for catalase activity. For the activity stability studies in serum, aliquots were tested at 0h, 0.25h, 1h, 2h, and 6h. Enzyme activities were calculated as the sample activity at a given timepoint divided by the initial sample activity at 0h.

2.11. OWH sample preparation for catalase activity stability

Slice culturing preparation for catalase activity stability studies were similar to LDH slice preparation, except supernatant was not exchanged at any timepoint after t = 0h. 100 μL of SCM containing free catalase was applied on top of slices, and 900 μL of normal SCM was applied below the membrane insert. Slices were collected at 0h, 2h, and 24h after catalase addition, homogenized with their supernatant, and immediately stored at −80 °C. Samples were thawed and assayed for catalase activity as described above.

2.12. Reduced glutathione (GSH) assay

For a subset of samples used for LDH supernatant collection, after the 24h timepoint, brain slices were immediately frozen at −80 °C for GSH detection with the GSH/GSSG ratio detection assay kit fluorometric green (Abcam). Following the manufacturer's instructions, 2 brain slices

approximating 20 g of brain tissue were homogenized in 400 μL of ice-cold mammalian lysis buffer composed of 0.5% NP-40 Surfact-Amps™ Detergent Solution (ThermoFisher) in PBS at pH 6.0 by pipetting up and down with a 200 μL pipetman. After centrifugation and transfer of supernatant to remove tissue debris, enzymes were removed by precipitating proteins with trichloroacetic acid (TCA), centrifugation, and pH neutralization with sodium bicarbonate following the Deproteinizing Sample Kit – TCA (Abcam). Sample supernatants were then diluted 10-fold in assay buffer. 50 μL of GSH standards and diluted sample supernatants were added to a 96-well plate, followed by the addition of 50 μL of GSH Assay Mixture (GAM) to each well while on ice. The 96-well plate was incubated for 60 m at room temperature in the dark, followed by 490/520 excitation/emission fluorescence measurement reading on a SpectraMax M5 UV–Vis Spectrophotometer (Molecular Devices) to measure the extent of thiol green indicator reaction with GSH. Adjusting for volume resuspension and dilutions, GSH concentrations were reported as μmoles GSH per gram of initial brain tissue.

2.13. Hydrogen nuclear magnetic resonance (H NMR) spectroscopy

1 mL non-loaded nanoparticles were frozen at −80 °C and lyophilized to a powder in a FreeZone 2.5 L −84 °C Benchtop Freeze Dryer (Labconco). Powdered nanoparticles were dissolved in 600 μL deuterated chloroform (MilliporeSigma) and added to 5 mm outer diameter economy NMR tubes (Wilmad-LabGlass). One sample per condition tested was scanned for 1H shifts relative to deuterated chloroform with a Bruker AV-300 NMR spectrometer. Measurements were run with 32 scans, recycle delay of 8, sweep width of 15, and time domain of 64k. Spectra were analyzed in Bruker CMC-assist software.

2.14. Differential scanning calorimetry

Analogous to the DE formulation process, 25 mg mPEG-OH (Creative PEGWorks) was dissolved in 1 mL DCM and sonicated with 200 μL DI for 0s, 30s, 60s, or 300s, followed by a second sonication of the same duration after the addition of 4 mL DI. Samples stir-incubated for 3h to evaporate off DCM, and were then frozen at −80 °C, and lyophilized to a powder in a FreeZone 2.5 L −84 °C Benchtop Freeze Dryer (Labconco). Between 4 and 6 mg of PEG lyophilized powder were added and sealed in Premium Hermetic Pan/Lid (DSC Consumables) sample holder. Samples underwent a heat/cool/heat/cool/heat ramp to a maximum temperature of 80 °C and minimum temperature of −60 °C with a ramp of 10 °C/min. The temperature at which the minimum heat flow occurred on the third heat ramp was recorded as the melting point temperature of the sample.

2.15. pH measurement

25 mg mPEG-OH (Creative PEGWorks) or no polymer was dissolved in 1 mL DCM, TCM, or EtAc and sonicated with 200 μL DI for 0s, 30s, or 300s, followed by a second sonication of the same duration after the addition of 4 mL DI. Samples stir-incubated for 3h to evaporate off organic solvent. pH was measured with an accumet pH meter (Fisher Scientific).

2.16. Statistics

For all experiments, normality was assumed, and significance was assessed using parametric unpaired t-tests with Welch's correction. All nanoparticle data with $n > 1$ are plotted as mean with standard error of the mean (SEM) error bars displayed on the graphs, unless they are too small to visualize. We reported statistical significance at two p-value levels: $p < 0.05$ (*) and $p < 0.001$ (**).

3. Results and discussion

3.1. Formulation optimization for nanoparticle enzyme activity and protection

With the end goal of maximizing therapeutic effect, it is important to optimize polymeric nanoparticle formulations to maximize enzyme loading. We first formulated catalase-loaded nanoparticles with either the DE method - varying sonication times – or the NPPT method, with CHA or PVA surfactants. For the DE method, sonication times of 15s, 30s, and 60s sonication times yielded similar sized nanoparticles for both CHA (58.4–70.8 nm) and PVA (109.8–113.3 nm) surfactants (Fig. 1A and B), while 1s sonication resulted in overall much larger diameters. The NPPT method also yielded larger nanoparticles than the 15–60s double emulsion nanoparticles. Importantly, except for the 1s DE and PVA NPPT conditions, all nanoparticle formulations were sub-114 nm in size. All nanoparticle formulations exhibited a near-neutral ζ-potential between 0 and -10 mV, as expected with a dense PEG coating (Fig. 1C and D). Nanoparticles with a sub-114 nm size and neutral surface charge exhibit rapid diffusion in the brain parenchyma [10,19,20].

We used catalase as a model enzyme for studying enzyme activity and degradation within the nanoparticle. CHA 30s sonication formulations exhibited an inverted U-trend with a significantly greater catalase activity of 45.2AU compared to all other CHA DE formulation activities (Fig. 1E and F). 30s sonication also exhibited the highest catalase activity of 80.1AU for PVA formulations, compared to the 1s, 60s, and NPPT activities. The active/total protein ratios present in the CHA nanoparticle formulations was also measured (Supplemental Fig. 1). 30s conditions had the highest active/total protein ratio among the DE conditions, but there was only a significant difference between 1s and 30s DE conditions ($p = 0.041$). Interestingly, the active/total protein ratio followed a similar trend as the total activity trend for the CHA nanoparticle formulations. It is likely that a minimum threshold sonication time is requisite to provide enough mixing to encapsulate enzyme and produce stable nanoparticles, with 1s formulations containing more aggregates and a larger diameter. On the other hand, excessive sonication time at 60s can lead to further enzyme deactivation due to more interaction time with high energy sonication waves and organic/aqueous interfaces. Scanning electron micrographs of 1s, 30s, and NPPT nanoparticles (Fig. 1G–I) confirm nanoparticle sizes as presented in Fig. 1A. Interestingly, the surface of the NPPT nanoparticles appears to be rougher than the DE formulations.

Bilati et al. previously characterized protein loading via DE and NPPT methods but did not assess enzymatic activity [21], which is crucial for determining nanoparticle protection of encapsulated protein. Catalase-loaded nanoparticle formulations were subsequently used for the catalase activity stability studies. We performed a catalase activity stability study over several hours in biologically relevant media at 37 °C for the catalase-loaded 30s sonication DE and NPPT formulations as well as for free catalase (Fig. 2). In the presence of 0.2 wt% pronase, a mixture of proteases from *Streptomyces griseus*, catalase-DE-nanoparticle activity was significantly greater than free catalase activity for all timepoints after t = 0h (Fig. 2A). After 2h of incubation with pronase, free catalase showed almost no measurable activity (2.9%), while CHA and PVA catalase-nanoparticles made via the 30s sonication DE method retained 75.7% and 18.6% activity, respectively. Even after 24h, CHA and PVA catalase-nanoparticles had 6.1% and 7.5% activity, respectively. The CHA DE retained significantly greater activity than the PVA DE activity at 1h, 2h, 4h, and 8h. NPPT with either CHA or PVA surfactant however provided no extension in catalase activity, decreasing to 5.4% ($p = 0.278$) and 2.5% ($p = 0.639$) activity, respectively, compared to free catalase activity of 2.1% at 4h (Fig. 2B). These results suggest that the high energy mixing during DE encapsulates catalase into the matrix interior of the nanoparticle where proteases cannot immediately penetrate. We suspect that the lack of high energy mixing results in only

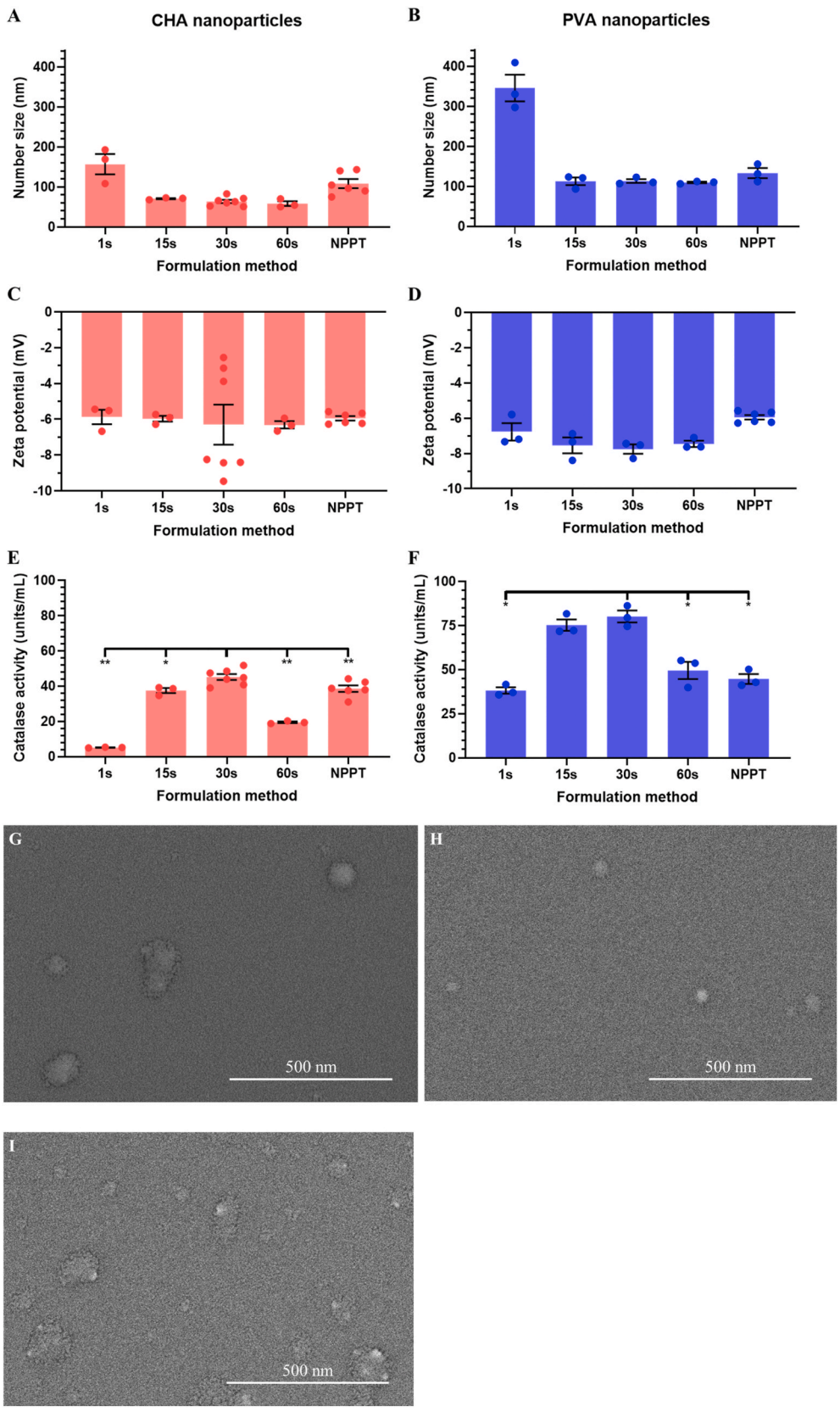

Fig. 1. Characteristics of catalase-loaded nanoparticles formulated with DE and NPPT methods. A) CHA and B) PVA nanoparticle number mean sizes, C) CHA and D) PVA nanoparticle ζ-potentials, and E) CHA and F) PVA nanoparticle catalase activities were determined for 1s, 15s, 30s, and 60s DE and NPPT formulations (n = 7 CHA DE 30s, n = 6 CHA NPPT, n = 3 all others). Data are reported as mean ± SEM. Scanning electron micrographs of nanoparticles formulated with CHA under the conditions of G) 1s DE, H) 30s DE, and I) NPPT.

surface-associated catalase for the NPPT formulation where the enzymes are still accessible and vulnerable to protease degradation. Our work is the first to exhibit this protective effect with polymeric nanoparticles under 100 nm in the presence of pronase, as well as in serum representative of degradative *in vivo* circulation conditions.

In the physiologically representative environment of serum extracted from rat blood, free catalase deactivated to 46.9% activity after incubating for 6h in serum, while catalase loaded within CHA nanoparticles

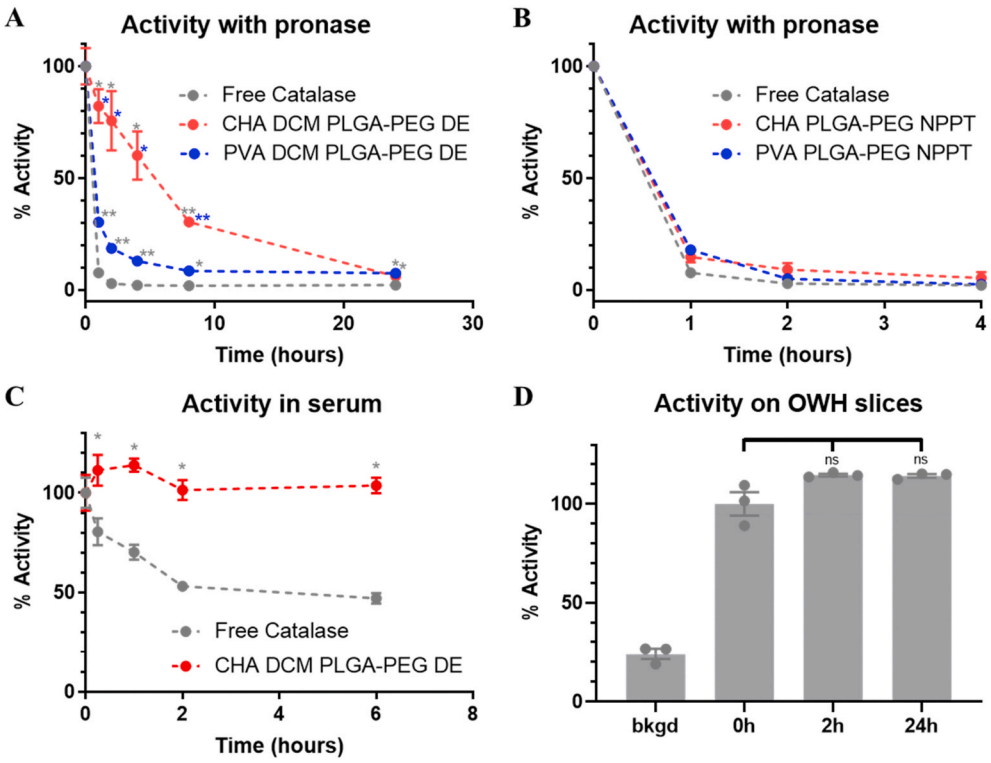

Fig. 2. Nanoparticle protection of catalase activity in biologically relevant environments. Free catalase and catalase-loaded nanoparticle activity in PBS with 0.2 wt% pronase at 37 °C A) over 24h for DE nanoparticles, and B) over 4h for NPPT nanoparticles. The same free catalase curve is presented for A) and B) for comparison. C) Free catalase and CHA DE nanoparticle activity over 6h in rat serum at 37 °C. For A) – C), at the respective timepoint, a grey * denotes compared to free catalase and a blue * denotes compared to PVA DE NP. D) Free catalase activity when incubated with OWH NT slices at 37 °C. The background condition (bkgd) represents the baseline catalase activity of the OWH slice without exogeneous catalase addition. The sample numbers are the following: n = 9 PVA DE NP in pronase conditions, n = 5 CHA NPPT NP in pronase conditions, n = 3 all other data. Data are reported as mean ± SEM. (For interpretation of the references to color in this figure legend, the reader is referred to the Web version of this article.)

exhibited no enzyme deactivation after 6h (Fig. 2C). Perhaps surprisingly, free catalase underwent no significant difference in activity between 0h and 2h ($p = 0.131$) or 24h ($p = 0.136$) when incubated with OWH slices directly, despite the documented presence of proteases in the brain (Fig. 2D) [22–24]. The peculiar but insignificant increase in catalase activity at 2h and 24h could be from improvement of the ox/redox environment with exogeneous catalase addition, increasing native catalase or glutathione peroxidase functions, obscuring the activity of exogenous catalase alone [25]. However, exploring the relative contributions of native hydrogen peroxide scavenging versus exogenous catalase addition was outside the scope of this work. The significant difference in catalase stability of free versus DE nanoparticle-encapsulated conditions in pronase and serum exemplifies the promising delivery improvements of DE polymeric nanoparticles for enzyme delivery. PLGA nanoparticles are widely studied for protein delivery, with the assumption that they are cargo-protective, but here we find that protective abilities are formulation method and surfactant-dependent, with NPPT providing no protection for the enzyme assessed in this study and CHA as a superior surfactant for enzyme protection.

3.2. *Biocompatibility screening of DE and NPPT nanoparticles*

Nanoparticle therapeutics administered to the brain encounter various neurological disease environments ranging from healthy tissue to regions of neuroinflammation or excitotoxicity [26]. To mimic these various environments, we used OWH slice models of LPS-induced neuroinflammation, MSG- and OGD-induced excitotoxicity, and NT healthy tissue. These OWH slices primarily consist of neurons, microglia, astrocytes, oligodendrocytes, pericytes, and endothelial cells, encompassing almost of the major cell types in the brain [27] – importantly these cells exist within a 3D architecture that mimics the *in vivo* local environment. We assessed the biocompatibility of non-loaded blank nanoparticle (bNP) formulations made via DE or NPPT with CHA as the surfactant on the four OWH slice models. On NT and LPS-exposed slices, neither DE nor NPPT bNPs significantly increased cytotoxicity (Fig. 3A and B). However, despite displaying the greatest protection of catalase activity, DCM PLGA-PEG DE bNPs significantly increased toxicities on the OWH models of excitotoxicity. For MSG-exposed slices there was a significant 1.7-fold increase in cytotoxicity upon addition of DE bNPs, while NPPT bNPs exhibited no effect (Fig. 3C). OGD-exposed slices exhibited the same trend with DE bNPs significantly increasing cytotoxicity 1.4-fold (Fig. 3D). 3h OGD-exposed slices elicited 1.8-fold lower cytotoxicity compared to 1000 mM MSG-exposure induced cytotoxicity. Similar to the need to assess each specific nanoparticle formulation for enzymatic cargo protection, thorough screening for biocompatibility is necessary for each formulation variant to ensure that a given nanoparticle formulation is not toxic in healthy or diseased environments. Fig. 3E–G shows immunofluorescence images of neurons for NT, 1000 mM MSG, and MSG + toxic DE bNPs, respectively. MAP2 colocalization with PI provides a qualitative assessment of neuronal viability. While MAP2+ neurons had cell nuclei lacking PI colocalization with an extended soma, 1000 mM MSG with or without DE bNP application resulted in dying or dead neurons with PI + cell nuclei and a retracted soma. MSG + DE bNP application further reduced neuronal soma area compared to neurons exposed to MSG alone.

We next sought to determine the cause of toxicity on MSG-exposed slices, starting with assessing the biocompatibility of the surfactants. 1% PVA had no significant effects on cytotoxicity on NT ($p = 0.394$) or MSG-exposed slices ($p = 0.419$), while 1% CHA caused a 5.2-fold increase for NT ($p < 0.001$), and 3.0-fold increase for MSG-exposed slices ($p = 0.001$) (Fig. 4A). However, upon evaluating the effects of nanoparticles made with PVA surfactant, we observed similar toxicity to that induced by CHA nanoparticles. PVA NPPT nanoparticles were inert, while PVA DE nanoparticles were highly toxic ($p = 0.005$) (Fig. 4B). In attempt to narrow down the toxic component of the system, we further assessed toxicity of control formulations and found that nanoparticles composed of PLGA polymer with PVA surfactant ($p = 0.072$), as well as sonicated PEG in DI/DCM and no surfactant elicited no change in toxicity ($p = 0.685$) (Fig. 4C). PVA PLGA-PEG bNPS emulsified in EtAc instead of DCM as the organic solvent also did not significantly increase cytotoxicity on MSG-exposed slices ($p = 0.188$) (Fig. 4C). In the presence

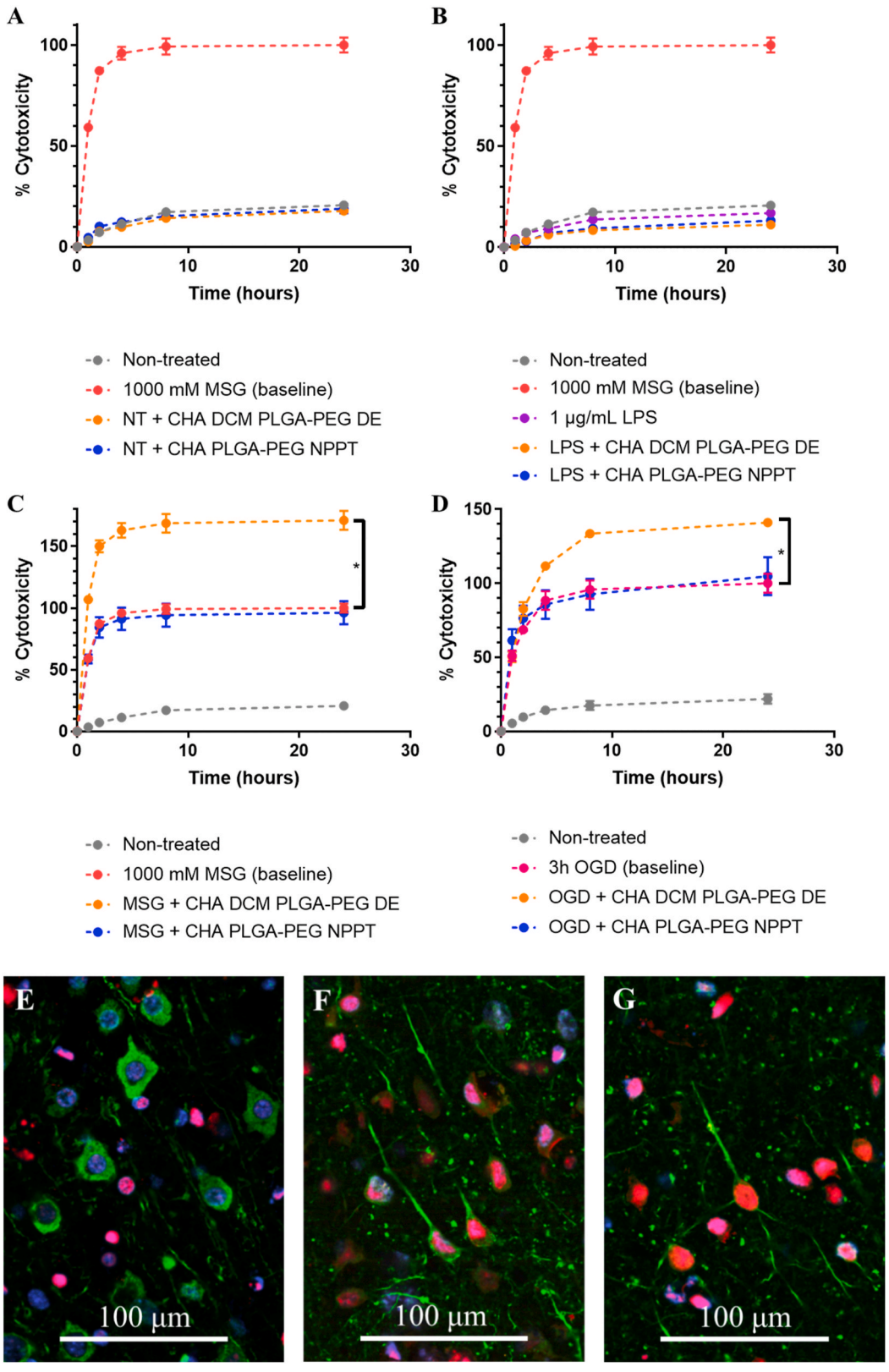

Fig. 3. Biocompatibility assessment of blank DE and NPPT nanoparticles. Percent cytotoxicity of A) non-treated (NT), B) LPS-exposed, C) MSG-exposed, and D) OGD-exposed slices after bNP application. For A) – C), cytotoxicity values are referenced to 1000 mM MSG as the 100% cytotoxicity baseline, and the NT and 1000 mM MSG curves are identical. For D), cytotoxicity values are referenced to 3h OGD as the 100% cytotoxicity baseline (n = 3). 100% cytotoxicity does not indicate that all cells are dead, hence some values are above 100%. Data are reported as mean ± SEM. Immunofluorescence of all cell nuclei stained with DAPI (blue), dead cell nuclei stained with PI (red), and neurons stained with MAP2 (green) for E) NT, F) 1000 mM MSG, and G) MSG + toxic DE bNP slices at t = 24h. Scale bars are 100 μm. (For interpretation of the references to color in this figure legend, the reader is referred to the Web version of this article.)

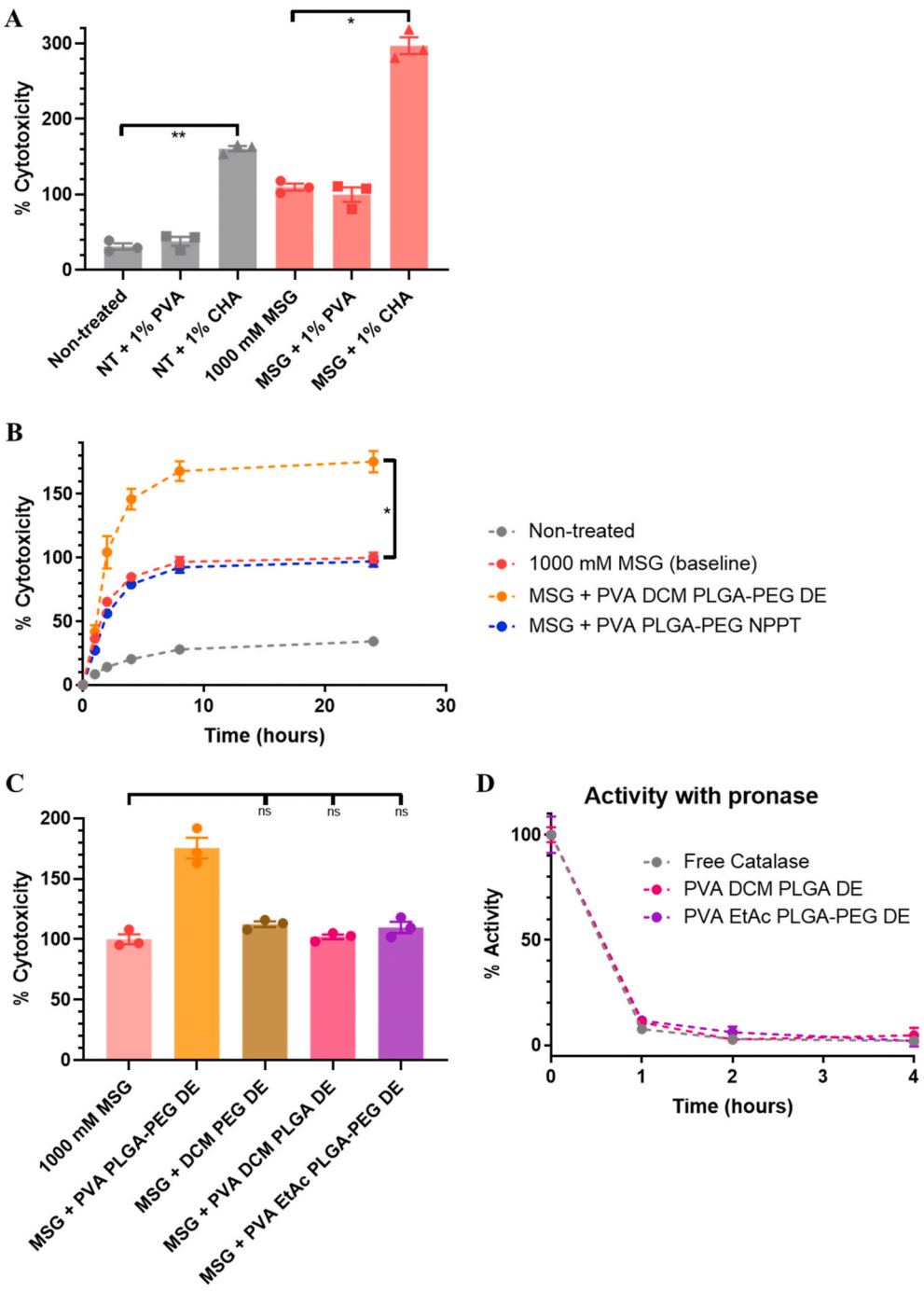

Fig. 4. Determination of toxicity from DE nanoparticles. Percent cytotoxicity of A) NT and MSG-exposed slices to PVA and CHA surfactant, B) MSG-exposed slices to PVA DE- and NPPT-bNPs, and C) MSG-exposed slices to 5k mPEG solution that underwent 60s DE in DI/DCM, PVA bNPs with PLGA instead of PLGA-PEG, and PVA bNPs formulated with EtAc instead of DCM as organic solvent at 24h. D) To evaluate enzymatic protection, catalase activity was measured for catalase-loaded PLGA nanoparticles and PLGA-PEG with EtAc nanoparticles in the presence of 0.2 wt% pronase in PBS at 37 °C (n = 3). Data are reported as mean ± SEM.

of pronase however, similar to other PVA formulations, PLGA with DCM and PLGA-PEG with EtAc formulations failed to provide any extension of catalase activity (Fig. 4D). Supplemental Fig. 2 displays the size, ζ-potential, and catalase activity characteristics of PLGA with DCM and PLGA-PEG with EtAc nanoparticle formulations. Thus, we concluded that the specific conditions of sonicated PLGA-PEG polymer dissolved in DCM organic solvent formulates nanoparticles with high toxicity on excitotoxic brain tissue. PLGA-PEG and DCM are popularly used in nanoparticle emulsion methodologies highlighting the importance of screening for unintentional toxicity [6,8,28]. Furthermore, PEG toxicity has previously been reported upon sonication of Pluronic surfactants that contain PEG chains during the synthesis of multi-walled carbon nanotubes [29].

3.3. *The role of oxidative stress in DCM PLGA-PEG DE nanoparticle toxicity*

Because the toxic DCM PLGA-PEG DE nanoparticles enhanced cytotoxicity on only MSG-exposed and OGD-exposed slices, but not NT or LPS-exposed slices, we investigated the mechanism of the excitotoxicity-induced vulnerability. It is documented that both MSG and OGD induce excitotoxicity-representative disease environments in organotypic *ex vivo* brain tissue [18,30]. Treatment of both MSG- and OGD-exposed slices with 0.1 mg superoxide dismutase (SOD) returned cytotoxicity levels to that of NT slices, confirming the role of superoxide-mediated oxidative stress in excitotoxicity (Fig. 5A). SOD application in addition to MSG + bNP exposure slices reduced cytotoxicity from 156.2% to 25.6%, which was still significantly greater than NT slice cytotoxicity of

11.3% ($p = 0.001$) (Fig. 5B). GSH concentrations were significantly different for all three conditions, with 1.29×10^{-5}, 3.47×10^{-5}, and 3.84×10^{-5} μmoles of GSH per gram of brain tissue for NT, MSG, and MSG + bNP slices, respectively (Fig. 5C). NT GSH levels were 3.7x greater than that of MSG ($p = 0.021$), while MSG + NP GSH levels were 1.1x greater than that of MSG ($p = 0.030$).

It is possible that with MSG exposure in combination with DCM PLGA-PEG bNP addition, the large dose of 0.1 mg SOD was inadequate for fully counteracting superoxide-induced damage. Generation of additional superoxide or other reactive oxygen species (ROS) would have elicited a further decrease in GSH levels as GSH is expended to scavenge ROS [31]. However, both MSG and MSG + bNP slices had similar GSH concentrations more than 3-fold less than the NT GSH level. Therefore, it is unlikely that the toxic nanoparticles increased the overall oxidative stress levels. The difference between NT versus MSG + bNP + SOD slice cytotoxicity (14.2%) was less than the difference between MSG versus MSG + bNP slice cytotoxicity (56.2%). We were unable to definitively identify whether the residual cytotoxicity difference between NT and MSG + bNP + SOD was due to MSG contributions, toxic nanoparticle contributions, or a combination of both. However, considering SOD fully inhibited MSG-induced cytotoxicity, we suspect that MSG-exposure with SOD treatment induced vulnerability to toxic bNP damage, but to a lesser extent than without SOD treatment. The DCM PLGA-PEG DE nanoparticles that were toxic on MSG- and OGD-exposed slices could be useful as protein delivery vehicles for inflammatory or regenerative environments without excessive ROS where they may not induce toxicity, or cancer applications where enhanced cancer cell death would be favorable.

3.4. Exploration of PEG degradation and toxic product formation

Furthermore, we explored whether the PEG chain of the nanoparticle underwent any reactions from the sonication process that could account for ROS-dependent toxicity. Probe sonication inputs high energy into liquid solution that can cause the formation and cavitation of vapor bubbles and subsequent production of high local temperature and pressure fluctuations that can split solvent molecules to form radicals [32–34]. These radicals can then react with PEG, leading to degradation via C–O chain scission and the formation of acid, alcohol, or aldehyde functional groups [29,35–37]. However, using H NMR we did not detect any characteristic shifts indicative of the presence of carboxylic acid, alcohol, or aldehyde functional groups. The NMR spectra looked identical for nanoparticles formulated via toxic conditions of 15s, 30s, and 300s PLGA-PEG DE sonication in DCM, and via non-toxic conditions of NPPT and 30s DE sonication in EtAc (Fig. 6A). In a model system of free PEG dissolved in DI/DCM, there was no decrease in melting temperature as a function of sonication time as determined by DSC (Fig. 6B). Since PEG melting temperature decreases with molecular weight, this indicated no significant PEG degradation had occurred [38,39]. Furthermore, there was no decrease in pH for DI/EtAc solutions with or without PEG (Fig. 6C), suggesting that no appreciable concentrations of formic acid or acetic acid, or other carboxylic acid degradation products formed as would be expected upon PEG degradation [40]. Instead, pH decreased as a function of sonication time for only DI/DCM solutions, independent of the presence of PEG (Fig. 6C), suggesting hydrochloric acid formation upon DCM degradation [34]. There are several potential explanations as to why we did not observe PEG degradation consistent with literature: (1) we studied free PEG alone instead of PEG as a copolymer with a hydrophobic segment such as in PLGA-PEG or Pluronic surfactants, (2) our sonication times of 30s are at least an order of magnitude shorter than the multiple minute- to hour-long sonication times explored in other studies, and (3) our sonication times are pulsed for 1s:1s on/off [29,36,37].

The mechanism as to how the DCM PLGA-PEG DE nanoparticles enact their cytotoxicity remains to be elucidated. To best gain insight into potential mechanisms of DCM-dependent toxicity, we compared the characteristics of DCM, EtAc, and TCM. Solvents with higher vapor pressure and lower surface tension undergo vapor bubble formation and subsequent cavitation at less extreme pressures [41,42]. Because DCM has the highest vapor pressure of the three solvents as calculated from

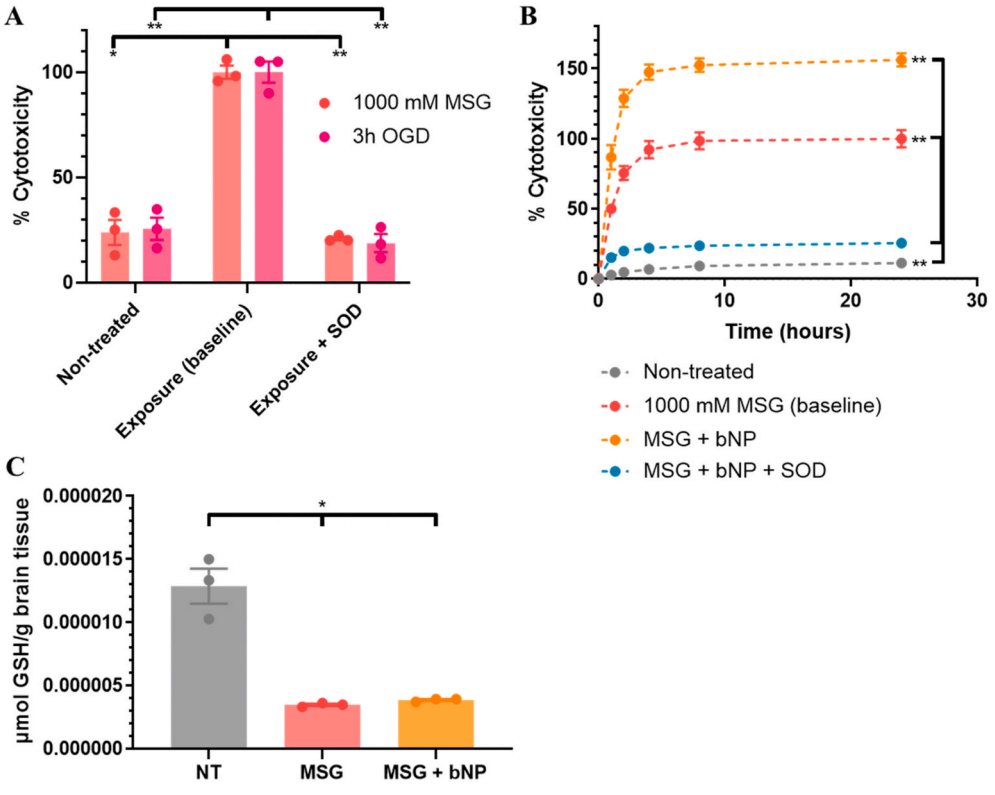

Fig. 5. The role of oxidative stress in CHA PLGA-PEG DE nanoparticle toxicity. Percent cytotoxicity of A) NT, MSG- or OGD-exposed, and MSG- or OGD-exposed with 0.1 mg SOD slices at 24h (n = 3), and B) NT, MSG-exposed, MSG-exposed with toxic DE bNPs, and MSG-exposed with toxic DE bNPs and 0.1 mg SOD slices (n = 3–4). C) GSH levels of NT, MSG-exposed, and MSG-exposed with bNPs slices at 24h (n = 3). bNP nanoparticles are formulated with CHA, DCM, and PLGA-PEG. Data are reported as mean ± SEM.

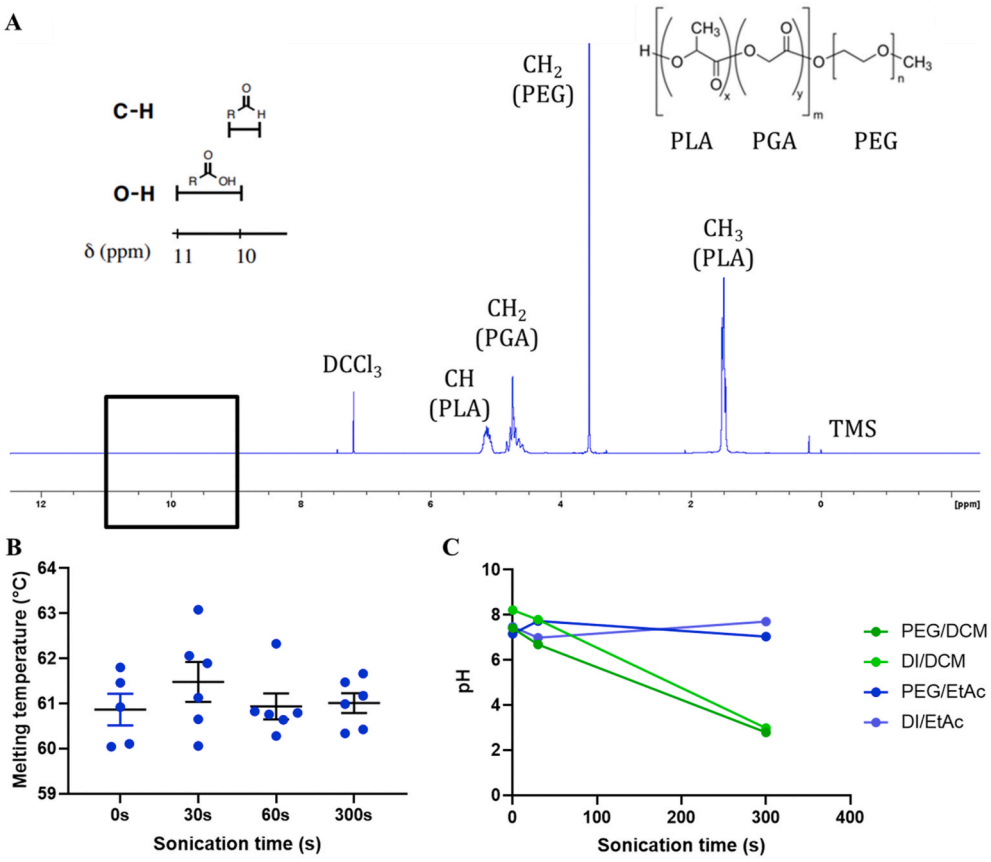

Fig. 6. Characterization methods to detect potential PEG degradation and toxic product formation. A) Representative H NMR spectrum of PLGA-PEG nanoparticles dissolved in deuterated chloroform, formulated via DE with sonication times of 15s, 30s, and 300s in DCM, and formulated via NPPT and 30s DE sonication in EtAc (n = 1). All profiles exhibited no differences and lacked the detection of carboxylic acid or aldehyde functional groups. B) Melting temperature of free PEG as a function of DE sonication time as determined by DSC (n = 5–6). Data are reported as mean ± SEM. C) pH as a function of DE sonication time for pure DI or PEG dissolved in DI/DCM or DI/EtAc and sonicated for 0s, 30s, or 300s (n = 1).

the Antoine equation (DCM: 353 mmHg, TCM 158 mmHg, EtAc 74 mmHg at 20 °C) [43], we speculate that under the nanoparticle formulation parameters used in our experiments, the sonication energy input was mild enough that cavitation only occurred with DCM as the organic solvent. Cavitation can induce the formation of reactive radical species for aqueous and organic solvents [44]. We propose that under DCM PLGA-PEG DE conditions, cavitation caused reactions with PLGA-PEG to yield currently unidentified toxic intermediates. Future work in organic solvent sonochemistry would be valuable to further investigate this theory. Nanoparticle toxicity is likely dependent on oxidative stress but may not exacerbate damage via increasing oxidative stress. There are a variety of potential mechanisms that remain to be explored, potentially involving excitotoxicity-induced altered behavior in the cellular uptake of nanoparticles, or nanoparticle upregulation of apoptotic or necrotic pathways. However, discerning the mechanism of toxicity may be challenging without first identifying a toxic molecular signature of the DCM PLGA-PEG DE nanoparticles.

Additionally, for future work, it is important to evaluate the toxicity of DCM PLGA-PEG DE nanoparticles *in vivo* on healthy, neuroinflammatory, and excitotoxic brain tissue, as well as the liver, kidney, and other organs. However, both intravenous and intracranial administration routes may need to be explored to determine if biocompatibility is dependent on total accumulation at sites within the brain microenvironment that have susceptible brain cells. We speculate that potential toxic byproducts associated with the toxic DE nanoparticle might get cleared or neutralized in circulation when administered systemically prior to reaching the brain, whereas local intracranial administration may pose a potential risk to oxidatively stressed brain cells.

3.5. Alternative biocompatible nanoparticle formulation conditions with enzymatic protection

We next investigated whether the addition of 5 mg free PEG during the sonication steps (PLGA-PEG + PEG) or replacement of DCM with TCM would yield biocompatible nanoparticles that protect enzymatic cargo. Both the addition of PLGA-PEG + PEG and TCM formulations elicited no significant change in cytotoxicity compared to MSG exposure alone ($p = 0.573$ and $p = 0.103$ respectively) (Fig. 7A). While sonicated PLGA-PEG causes toxicity, free PEG holds characteristics that could improve formulation conditions and account for the elimination of nanoparticle-mediated toxicity. Due to PEG miscibility in both water and DCM, PEG readily diffuses to the aqueous/organic interfaces and also competitively occupies the interface to reduce protein denaturation [45]. It is possible that the presence of free PEG at the interface could substitute for the PLGA-PEG co-block and undergo the unknown toxicity-inducing reaction, followed by subsequent washout of PEG-scapegoat, yielding biocompatible nanoparticles from the PLGA--PEG + PEG formulation condition. Both PLGA-PEG + PEG and TCM formulations also exhibited higher enzyme activity compared to free catalase at every measured timepoint across 24h in the presence of 0.2 wt% pronase, with a final percent initial activity of 30.6% ($p < 0.001$) for PLGA-PEG + PEG and 32.1% ($p < 0.001$) for TCM (Fig. 7B). Similar formulation conditions to the enzyme-protecting DCM PLGA-PEG formulation, but with the addition of free PEG or replacement of DCM with TCM, could account for the retention of enzyme protective capabilities.

In attempt to further elucidate the role of additional free PEG incorporation in the formulation, we assessed nanoparticle cytotoxicity of bNPs with 5 mg free PEG added to the formulation after the sonication steps in the aqueous sink phase (PEG_S), bNPs with 5 mg free PEG added to the final 1 mL nanoparticle resuspension in PBS (PEG_F), and free PEG

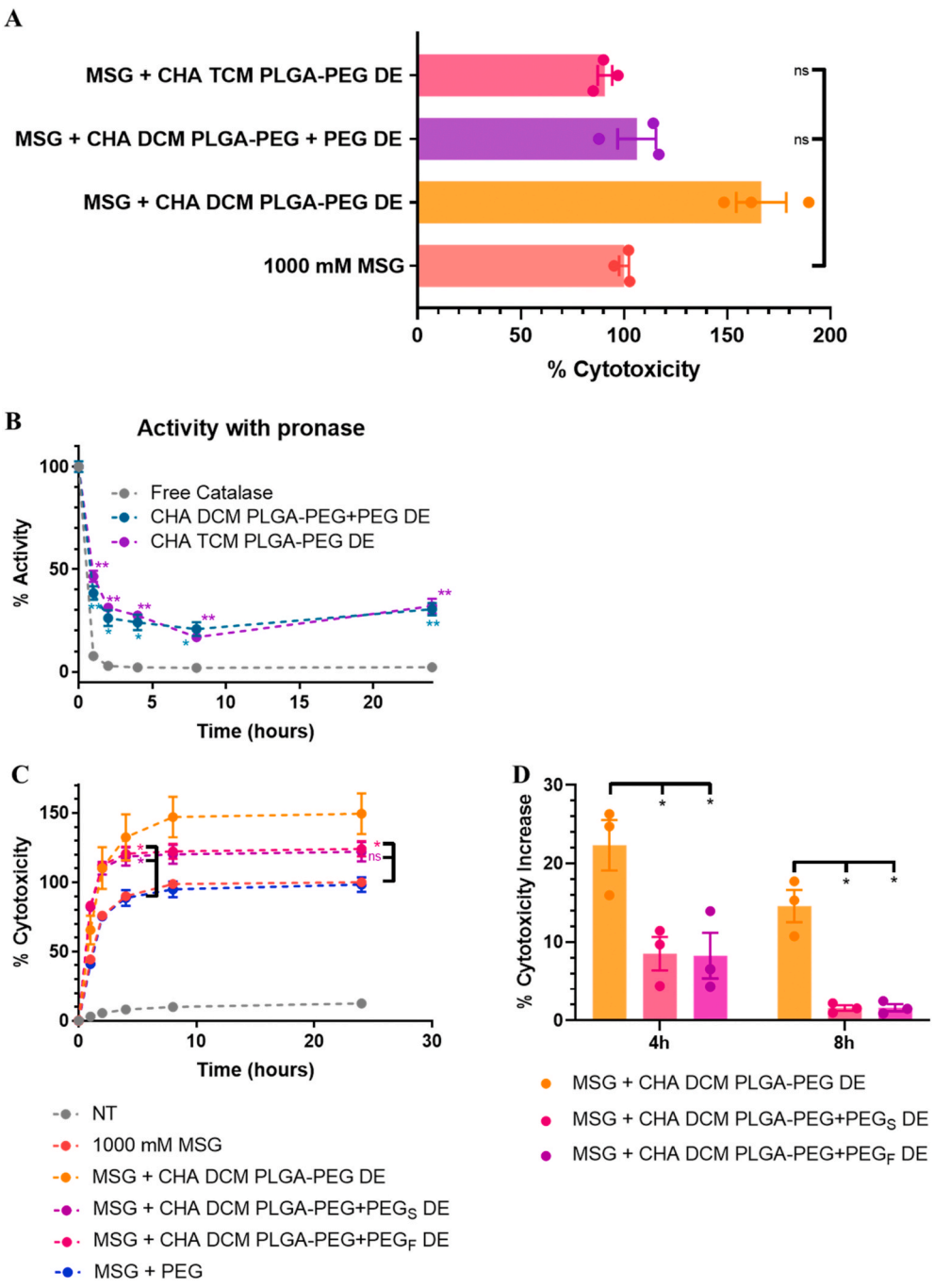

Fig. 7. Identification of non-toxic DE nanoparticles with enzymatic protection. Percent cytotoxicity of A) MSG-exposed slices with the addition of PLGA-PEG nanoparticles with 5 mg PEG added during the sonication steps and PLGA-PEG nanoparticles formulated with TCM instead of DCM at 24h (n = 3), and B) the catalase activity of PLGA-PEG + PEG and PLGA-PEG with TCM nanoparticles in the presence of 0.2 wt% pronase in PBS over 24 h at 37 °C (n = 6). Percent cytotoxicity of C) MSG-exposed slices with the addition of bNPs with 5 mg PEG added during the final resuspension (PEG_F), or sink phase (PEG_S), or 5 mg PEG alone (n = 3), and D) the percent cytotoxicity increase of the toxic PLGA-PEG, PEG_F, and PEG_S bNP supernatants at 4h and 8h (n = 3). Data are reported as mean ± SEM.

alone. PEG_S and PEG_F conditions exhibited intermediate toxicities of 121.8% and 124.0% respectively between 1000 mM MSG alone (100%) and MSG with toxic bNP addition (149.4%), while MSG with free PEG alone exhibited no significant difference in cytotoxicity from MSG exposure alone ($p = 0.767$) (Fig. 7C). However, at 24h timepoint only PEG_F cytotoxicity was significantly different from MSG alone ($p = 0.034$) while PEG_S cytotoxicity differences trended towards significance ($p = 0.075$). Interestingly, compared at the 4h earlier timepoint, PEG_S and PEG_F were both significantly greater than MSG alone ($p = 0.037$ and $p = 0.014$ respectively) (Fig. 7C). PEG_S and PEG_F cytotoxicity were not significantly different from MSG with toxic bNP addition at 24h ($p = 0.191$ and $p = 0.217$ respectively) (Fig. 7C), however the differences in percent cytotoxicity increase at 4h ($p = 0.029$ and $p = 0.032$ respectively) and 8h ($p = 0.021$ and $p = 0.020$ respectively) were significant (Fig. 7D). Size, ζ-potential, and catalase activity characteristics of the PLGA-PEG + PEG with DCM and the PLGA-PEG with TCM formulations, and the size and ζ-potential characteristics of PEG_S and PEG_F bNPs are provided in Supplemental Fig. 3. It is possible that free PEG is still incorporated into the nanoparticle matrix for the PLGA-PEG + PEG, PEG_S, and PEG_F formulations. If so, free PEG could reduce cytotoxicity by enhancing axonal repair, with studies demonstrating the neuroprotective ability of PEG in spinal cord injury and severe TBI *in vivo* via promoting cell membrane repair [46,47]. Further exploration is needed to understand the exact mechanisms as to why PEG addition or TCM replacement results in nontoxic nanoparticle formulations. Regardless these formulations provide promising alternatives for biocompatible, enzyme-protecting polymeric nanoparticles for the treatment of excitotoxicity in neurological diseases.

4. Conclusion

There is an urgent demand for therapeutics against neurological disease, and a high interest in the therapeutic potential of enzymes. The use of polymeric nanoparticle carriers is highly promising for enzyme delivery to the brain with their ability to bypass many obstacles to therapeutic delivery to the brain injury target site. We found an optimal sonication time of 30s for the DE formulation method to maximize enzymatic activity loading. As evidenced in the presence of pronase and in rat blood derived serum, catalase-loaded CHA DCM PLGA-PEG DE nanoparticles extended catalase activity across several hours while free catalase and catalase-loaded NPPT nanoparticles rapidly deactivated. However, independent of surfactant, DCM PLGA-PEG DE nanoparticles were also highly toxic on MSG- and OGD-exposed OWH brain slice models of excitotoxicity, but not on NT or LPS-exposed slices. A dense PEG coating for stealth-imbuing properties is requisite for an effective therapeutic but was also found to be a source of nanoparticle toxicity in DE formulations. We elucidated the role of oxidative stress in the vulnerability of excitotoxicity-induced OWH slices but found that the toxic DCM PLGA-PEG DE nanoparticles did not further increase oxidative stress, and that there was no indication of PEG degradation. Interestingly, incorporation of free PEG in addition to the PLGA-PEG in DCM during the DE sonication steps or replacement of DCM with TCM as the organic solvent yielded non-toxic nanoparticle formulations on MSG-exposed slices that still effectively extended catalase activity across 24h. Polymeric PLGA-PEG nanoparticles formulated via the DE method present an effective strategy for enzyme delivery against neurological diseases, but these formulations must be thoroughly screened to ensure protective capabilities and biocompatibility.

Funding

This work was supported by the Burroughs Wellcome Fund Career Award at Scientific Interfaces (Grant #1013937) and the National Institute of General Medical Sciences (Grant #R35GM124677). BWF and NIGMS were not involved in the conduct of research, analysis, or writing of the report.

Declaration of competing interest

The authors declare they have no conflict of interest.

Acknowledgements

Part of this work was conducted at the Molecular Analysis Facility, a National Nanotechnology Coordinated Infrastructure site at the University of Washington which is supported in part by the National Science Foundation (grant NNCI-1542101), the University of Washington, the Molecular Engineering & Sciences Institute, and the Clean Energy Institute. Specifically, the authors would like to thank Research Scientist Scott Braswell for assistance with scanning electron microscopy. The authors would like to thank the UW Department of Chemistry NMR Facility and the Associate Manager Dr. Adrienne Roehrich for assistance with H NMR data acquisition design. The authors would also like to thank the UW Department of Chemical Engineering Bindra Lab for access to the Differential Scanning Calorimeter and Malvern Zetasizer.

Appendix A. Supplementary data

Supplementary data to this article can be found online at https://doi.org/10.1016/j.biomaterials.2020.120238.

References

[1] J. Kreuter, Drug delivery to the central nervous system by polymeric nanoparticles: what do we know? Adv. Drug Deliv. Rev. 71 (2014) 2–14.
[2] C. Vauthier, K. Bouchemal, Methods for the preparation and manufacture of polymeric nanoparticles, Pharm. Res. (N. Y.) 26 (5) (2009) 1025–1058.
[3] T. Patel, et al., Polymeric nanoparticles for drug delivery to the central nervous system, Adv. Drug Deliv. Rev. 64 (7) (2012) 701–705.
[4] T.D. Dziubla, A. Karim, V.R. Muzykantov, Polymer nanocarriers protecting active enzyme cargo against proteolysis, J. Contr. Release 102 (2) (2005) 427–439.
[5] B. Petri, et al., Chemotherapy of brain tumour using doxorubicin bound to surfactant-coated poly(butyl cyanoacrylate) nanoparticles: revisiting the role of surfactants, J. Contr. Release 117 (1) (2007) 51–58.
[6] K. Avgoustakis, Pegylated poly(lactide) and poly(lactide-co-glycolide) nanoparticles: preparation, properties and possible applications in drug delivery, Curr. Drug Deliv. 1 (4) (2004) 321–333.
[7] I. Bala, S. Hariharan, M.N. Kumar, PLGA nanoparticles in drug delivery: the state of the art, Crit. Rev. Ther. Drug Carrier Syst. 21 (5) (2004) 387–422.
[8] E. Locatelli, M.C. Franchini, Biodegradable PLGA-b-PEG polymeric nanoparticles: synthesis, properties, and nanomedical applications as drug delivery system, J. Nanoparticle Res. 14 (12) (2012) 1316.
[9] E. Sah, H. Sah, Recent trends in preparation of poly (lactide-co-glycolide) nanoparticles by mixing polymeric organic solution with antisolvent, J. Nanomater. (2015) 2015.
[10] E.A. Nance, et al., A dense poly (ethylene glycol) coating improves penetration of large polymeric nanoparticles within brain tissue, Sci. Transl. Med. 4 (149) (2012), 149ra119-149ra119.
[11] A. Patel, et al., Recent advances in protein and Peptide drug delivery: a special emphasis on polymeric nanoparticles, Protein Pept. Lett. 21 (11) (2014) 1102–1120.
[12] P. Langguth, et al., The challenge of proteolytic enzymes in intestinal peptide delivery, J. Contr. Release 46 (1–2) (1997) 39–57.
[13] V.R. Muzykantov, Targeting of superoxide dismutase and catalase to vascular endothelium, J. Contr. Release 71 (1) (2001) 1–21.
[14] W.M. Pardridge, The blood-brain barrier: bottleneck in brain drug development, NeuroRx 2 (1) (2005) 3–14.
[15] K. Kalantar-zadeh, et al., Two-dimensional transition metal dichalcogenides in biosystems, Adv. Funct. Mater. 25 (32) (2015) 5086–5099.
[16] C.V. Rahman, et al., PLGA/PEG-hydrogel composite scaffolds with controllable mechanical properties, J. Biomed. Mater. Res. B Appl. Biomater. 101 (4) (2013) 648–655.
[17] R.F. Beers, I.W. Sizer, A spectrophotometric method for measuring the breakdown of hydrogen peroxide by catalase, J. Biol. Chem. 195 (1) (1952) 133–140.
[18] R. Liao, T.R. Wood, E. Nance, Superoxide dismutase reduces monosodium glutamate-induced injury in an organotypic whole hemisphere brain slice model of excitotoxicity, J. Biol. Eng. 14 (2020) 3.
[19] E. Nance, et al., Non-invasive delivery of stealth, brain-penetrating nanoparticles across the blood-brain barrier using MRI-guided focused ultrasound, J. Contr. Release 189 (2014) 123–132.
[20] C. Zhang, et al., Convection enhanced delivery of cisplatin-loaded brain penetrating nanoparticles cures malignant glioma in rats, J. Contr. Release 263 (2017) 112–119.
[21] U. Bilati, E. Allemann, E. Doelker, Nanoprecipitation versus emulsion-based techniques for the encapsulation of proteins into biodegradable nanoparticles and process-related stability issues, AAPS PharmSciTech 6 (4) (2005) 594–604.
[22] Y. Wang, W. Luo, G. Reiser, Trypsin and trypsin-like proteases in the brain: proteolysis and cellular functions, Cell. Mol. Life Sci. 65 (2) (2008) 237–252.
[23] A. Pope, R.A. Nixon, Proteases of human brain, Neurochem. Res. 9 (3) (1984) 291–323.
[24] C. Cao, et al., Catalase is regulated by ubiquitination and proteosomal degradation. Role of the c-Abl and Arg tyrosine kinases, Biochemistry 42 (35) (2003) 10348–10353.
[25] M. Mokni, et al., Effect of resveratrol on antioxidant enzyme activities in the brain of healthy rat, Neurochem. Res. 32 (6) (2007) 981–987.
[26] N. Quillinan, P.S. Herson, R.J. Traystman, Neuropathophysiology of brain injury, Anesthesiol. Clin. 34 (3) (2016) 453–464.
[27] C. Humpel, Organotypic brain slice cultures: a review, Neuroscience 305 (2015) 86–98.
[28] Y. Li, et al., PEGylated PLGA nanoparticles as protein carriers: synthesis, preparation and biodistribution in rats, J. Contr. Release 71 (2) (2001) 203–211.
[29] R. Wang, et al., Generation of toxic degradation products by sonication of Pluronic (R) dispersants: implications for nanotoxicity testing, Nanotoxicology 7 (7) (2013) 1272–1281.
[30] H. Cimarosti, J.M. Henley, Investigating the mechanisms underlying neuronal death in ischemia using in vitro oxygen-glucose deprivation: potential involvement of protein SUMOylation, Neuroscientist 14 (6) (2008) 626–636.
[31] C.C. Winterbourn, Revisiting the reactions of superoxide with glutathione and other thiols, Arch. Biochem. Biophys. 595 (2016) 68–71.
[32] S. Ziembowicz, M. Kida, P. Koszelnik, Sonochemical formation of hydrogen peroxide, in: Multidisciplinary Digital Publishing Institute Proceedings, 2017.
[33] B. Miljevic, et al., To sonicate or not to sonicate PM filters: reactive oxygen species generation upon ultrasonic irradiation, Aerosol. Sci. Technol. 48 (12) (2014) 1276–1284.
[34] A. Chiba, T. Furugori, W.-C. Wu, Ultrasonic decomposition of dichloromethane, J. Surf. Finish. Soc. Jpn. 45 (7) (1994) 735–738.
[35] H. Kaczmarek, L. Lindén, J. Rabek, Reactions of hydroxyl (HO•) and hydroperoxyl (HO) radicals generated chemically and photochemically with poly (ethylene oxide), J. Polym. Sci. Polym. Chem. 33 (6) (1995) 879–890.

[36] H. Kawasaki, Y. Takeda, R. Arakawa, Mass spectrometric analysis for high molecular weight synthetic polymers using ultrasonic degradation and the mechanism of degradation, Anal. Chem. 79 (11) (2007) 4182–4187.
[37] S. Vijayalakshmi, G. Madras, Effect of initial molecular weight and solvents on the ultrasonic degradation of poly (ethylene oxide), Polym. Degrad. Stabil. 90 (1) (2005) 116–122.
[38] K. Pielichowski, K. Flejtuch, Differential scanning calorimetry studies on poly (ethylene glycol) with different molecular weights for thermal energy storage materials, Polym. Adv. Technol. 13 (10–12) (2002) 690–696.
[39] R. Majumdar, K. Alexander, A. Riga, Physical characterization of polyethylene glycols by thermal analytical technique and the effect of humidity and molecular weight, Die Pharmazie-An International Journal of Pharmaceutical Sciences 65 (5) (2010) 343–347.
[40] J.A. Giroto, et al., Degradation of poly (ethylene glycol) in aqueous solution by photo-Fenton and H2O2/UV processes, Ind. Eng. Chem. Res. 49 (7) (2010) 3200–3206.
[41] Q. Cheng, et al., Ultrasound-assisted SWNTs dispersion: effects of sonication parameters and solvent properties, J. Phys. Chem. C 114 (19) (2010) 8821–8827.
[42] E. Camerotto, et al., Influence of surface tension on cavitation noise spectra and particle removal efficiency in high frequency ultrasound fields, J. Appl. Phys. 112 (11) (2012) 114322.
[43] G.W. Thomson, The antoine equation for vapor-pressure data, Chem. Rev. 38 (1) (1946) 1–39.
[44] P. Riesz, D. Berdahl, C. Christman, Free radical generation by ultrasound in aqueous and nonaqueous solutions, Environ. Health Perspect. 64 (1985) 233–252.
[45] A. Malzert-Fréon, J.-P. Benoît, F. Boury, Interactions between poly (ethylene glycol) and protein in dichloromethane/water emulsions: a study of interfacial properties, Eur. J. Pharm. Biopharm. 69 (3) (2008) 835–843.
[46] J. Luo, R. Borgens, R. Shi, Polyethylene glycol improves function and reduces oxidative stress in synaptosomal preparations following spinal cord injury, J. Neurotrauma 21 (8) (2004) 994–1007.
[47] A.O. Koob, et al., Intravenous polyethylene glycol inhibits the loss of cerebral cells after brain injury, J. Neurotrauma 22 (10) (2005) 1092–1111.